

Algorithms in Array Signal Processing

A Project Report

submitted by

SRIKANTH KUTHURU

*in partial fulfilment of the requirements
for the award of the degree of*

BACHELOR OF TECHNOLOGY



**DEPARTMENT OF ELECTRICAL ENGINEERING
INDIAN INSTITUTE OF TECHNOLOGY MADRAS.**

MAY 2016

THESIS CERTIFICATE

This is to certify that the thesis titled **Algorithms in Array Signal Processing**, submitted by **Srikanth Kuthuru**, to the Indian Institute of Technology, Madras, for the award of the degree of **Bachelor of Technology**, is a bona fide record of the research work done by him under our supervision. The contents of this thesis, in full or in parts, have not been submitted to any other Institute or University for the award of any degree or diploma.

Srikrishna Bhashyam
Professor
Dept. of Electrical Engineering
IIT-Madras, 600 036

Place: Chennai

Date: 3rd May 2016

ACKNOWLEDGEMENTS

I would first like to thank my thesis advisor Prof.Srikrishna Bhashyam of Indian Institute of Technology, Madras for his valuable suggestions throughout the project. I thank my parents and friends for their continuous support and encouragement. This accomplishment would not have been possible without them.

Thank you,
Srikanth Kuthuru

ABSTRACT

The field of array signal processing has been widely studied and has numerous applications in RADAR systems, SONAR, Radio astronomy, Seismology, Medical diagnosis and communication systems. This thesis analyses various algorithms from array processing literature which are used for direction of arrival estimation. A brief introduction to signal model and sensor array structures is provided at the beginning. Basic beamforming techniques like conventional beamformer, MVDR beamformer and delay-sum beamformer are discussed with the help of graphical measures. Next, high resolution algorithms like MUSIC and ESPRIT are discussed and their performance is compared with beamforming algorithms. Recent work on Nested arrays (Pal and Vaidyanathan, 2010) has gained significant fame in the field of array signal processing. Nested array is an array geometry through which it is possible to detect $O(N^2)$ sources with only N sensors which is not possible with traditional Uniform Linear Arrays(ULA). An algorithm based on spatial smoothing and MUSIC for nested arrays has been mentioned in (Pal and Vaidyanathan, 2010). Here we develop a new algorithm using spatial smoothing and ESPRIT and compare both the results. We will show that ESPRIT is considerably faster than MUSIC while maintaining almost the same RMSE.

TABLE OF CONTENTS

ACKNOWLEDGEMENTS	i
ABSTRACT	ii
LIST OF FIGURES	vi
ABBREVIATIONS	vii
1 INTRODUCTION	1
1.1 Background and Formulation	2
2 Beamforming	6
2.1 Delay Sum Beamforming	6
2.2 Conventional Narrow band beamforming	7
2.3 Minimum Variance Distortionless Response (MVDR) Beamformer or Capon Beamformer:	9
2.4 Simulations	10
3 Subspace Methods	12
3.1 MUSIC	12
3.1.1 Algorithm	14
3.1.2 Simulations	14
3.2 ESPRIT	16
3.2.1 Algorithm	18
3.2.2 Simulations	20

4	Nested Arrays	21
4.1	Algorithm Formulation	23
4.2	Simulation System Model	27
4.2.1	Sensor Array Structure	27
4.2.2	Co-Array structure	27
4.3	Simulations	29
4.3.1	Conclusions	35

LIST OF FIGURES

1.1	6 element ULA with spacing = d and 2 far-field sources s_1, s_2 .	3
1.2	Magnitude Response	5
1.3	Spatial Aliasing	5
2.1	Delay-sum beamformer	7
2.2	MVDR vs Conventional Beamformer, 9 sensors	10
2.3	MVDR vs Conventional Beamformer, Resolution plot	11
3.1	SNR = 5dB, Src angles = 30,100, 9 sensors	15
3.2	SNR = 5dB, Src angles = 30,50, 9 sensors	15
3.3	ESPRIT sensor array geometry	17
3.4	SNR=10dB, 9 sensors, ESPRIT = 18 sensors, angles = 65,85 . .	20
4.1	Nested Array	28
4.2	Co-Array	28
4.3	Histogram of source angles observed by 6 element nested array with SS-rootMUSIC and SS-ESPRIT algorithms, $T = 9600$. . .	30
4.4	Histogram of source angles observed by 6 element nested array with SS-rootMUSIC and SS-ESPRIT algorithms, $T = 800$. . .	30
4.5	RMSE of source angles w.r.t SNR as observed by a 6 element nested array with SS-rootMUSIC and SS-ESPRIT algorithms and as observed by a 12-element ULA with rootMUSIC algorithm, T = 9600	31

4.6	RMSE of source angles w.r.t SNR as observed by a 6 element nested array with SS-rootMUSIC and SS-ESPRIT algorithms and as observed by a 12-element ULA with rootMUSIC algorithm, $T = 800$	31
4.7	Time taken by both the algorithms after feeding in the covariance matrices. ESPRIT is faster than rootMUSIC.	32
4.8	Time taken by both the algorithms which includes the estimation of covariance matrices also. ESPRIT is faster than rootMUSIC. .	33
4.9	RMSE performance comparison between ULA and Nested array with 6 sensors each.	34

ABBREVIATIONS

IITM	Indian Institute of Technology, Madras
RADAR	RAdio Detection and Ranging
SONAR	SOund NAvigation and Ranging
ULA	Uniform Linear Array
doa	Direction of Arrival
MVDR	Minimum Variance Distortionless Response
MUSIC	MUltiple SIgnal Classification
ESPRIT	Estimation of Signal Parameters via Rotational Invariance Techniques

CHAPTER 1

INTRODUCTION

Array signal processing is a wide area of research that embodies techniques to solve 1-D signal to multi-dimensional signal processing problems. Array sensor structure can be interpreted as a set of sensors (eg. Antennas, microphones) that are spatially separated. One of the basic problems that can be solved using array processing is determining directions of incoming sources. This area is centered on the ability of using and combining data from different sensors in order to deal with a specific estimation task. Array processing techniques are used in RADAR, SONAR, Radio astronomy, Medical diagnosis, Seismology, anti-jamming and wireless communications.

Looking into the field of communications, antenna arrays have emerged as a support technology to increase the spectral efficiency and enhance the accuracy of wireless communication systems by utilizing spatial dimension in addition to time and frequency dimensions. The multiuser - medium multiple access - and multipath - signal propagation over multiple scattering paths in wireless channels- communication model is one of the most widespread communication models in wireless communication. In multiuser communication environment, the existence of multiuser increases the inter-user interference possibility that can affect quality and performance of the system adversely. In mobile communication systems the multipath problem is one of the basic problems that base stations have to deal with. Base stations use an antenna array of several elements to achieve higher selectivity i.e better spatial diversity. Receiving array

can be directed in the direction of one user at a time, while avoiding the interference from other users.

There are 4 assumptions made and are followed throughout the thesis. The first assumption is that there is uniform propagation in all directions of isotropic and non-dispersive medium. The second assumption is that for far field array processing, the radius of propagation is much greater than size of the array and that they seem like plane waves to the sensor array. The third assumption is that there is AWGN, signal and noise are uncorrelated. Finally, the last assumption is that there are no calibration issues.

(Johnson and Dudgeon, 1992) and (Van Trees, 2004) have been very useful for reference throughout the thesis.

1.1 Background and Formulation

General Plane Wave equation in Space-Time domain:

$$s(\vec{x}, t) = \exp(j(\omega_0 t - \vec{k}^0 \cdot \vec{x}))$$

\vec{k}^0 =direction of propagation

ω_0 =frequency of the wave

4D Transform:

Transformation from space-time domain to wavenumber-frequency domain.

$$S(\vec{k}, \omega) = \int_{-\infty}^{\infty} s(\vec{x}, t) e^{-j(\omega t - \vec{k} \cdot \vec{x})} d\vec{x} dt$$

$$\vec{k} = k_x \hat{i} + k_y \hat{j} + k_z \hat{k}$$

$\vec{k} \implies$ 3-D wave vector

$\omega \implies$ Temporal frequency variable

Sensor Arrays:

Sensor arrays receive signals at fixed points in space where they are located.

Sensor arrays are characterized by Aperture functions. These can be viewed as spatial filters for which the plane waves are the input and the perceived signal by the sensor system as the output.

$$w(\vec{x}) \longleftrightarrow W(\vec{k})$$

$$W(\vec{k}) = \int_{-\infty}^{\infty} w(\vec{x}) e^{j\vec{k} \cdot \vec{x}}$$

Uniform Linear Array (ULA):

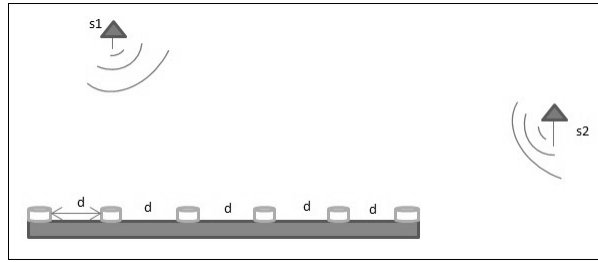


Figure 1.1: 6 element ULA with spacing = d and 2 far-field sources s1, s2

M sensor linear array , M=odd

$$b(x) = \sum_{m=-\frac{M-1}{2}}^{\frac{M-1}{2}} \delta(x - md)$$

$$w(\vec{x}) = b(x)\delta(y)\delta(z)$$

Since the ULA is placed in the x-direction only k_x component comes into the final equation.

$$W(k_x) = \frac{\frac{\sin(k_x Md)}{2}}{\frac{\sin(k_x d)}{2}}$$

Polar form:

\vec{k} can be represented in polar form.

$$k_x = k_r \sin(\phi) \cos(\theta)$$

$$k_y = k_r \sin(\phi) \sin(\theta)$$

$$k_z = k_r \cos(\phi)$$

For example: Consider the above aperture function

$$W(k_x) = \frac{\frac{\sin(k_x M d)}{2}}{\sin(k_x d)}$$

$$W(k_r, \phi, \theta) = \frac{\sin\left(\frac{k_r M d \sin(\phi) \cos(\theta)}{2}\right)}{\sin\left(\frac{k_r d \sin(\phi) \cos(\theta)}{2}\right)}$$

Example Plot: Fig. 1.2

Let $\theta = 0$ and ϕ varies from $0 - \frac{\pi}{2}$

$$W\left(\frac{2\pi}{\lambda}, \phi, 0\right) = \frac{\sin\left(\frac{M d \pi \sin(\phi)}{\lambda}\right)}{\sin\left(\frac{d \pi \sin(\phi)}{\lambda}\right)}$$

Spatial Aliasing:

distance between the sensors =d

$d \leq \frac{\lambda}{2}$ for no spatial aliasing

Example plot where $d = \lambda$ and spatial aliasing takes place: Fig. 1.3

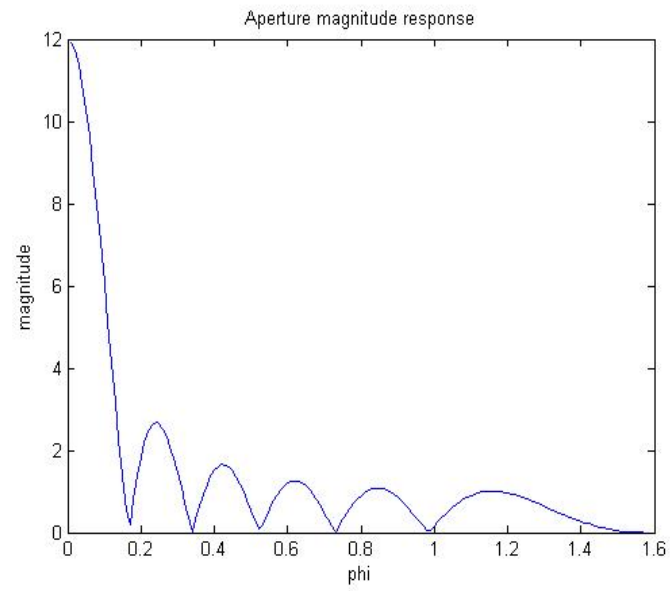


Figure 1.2: Magnitude Response

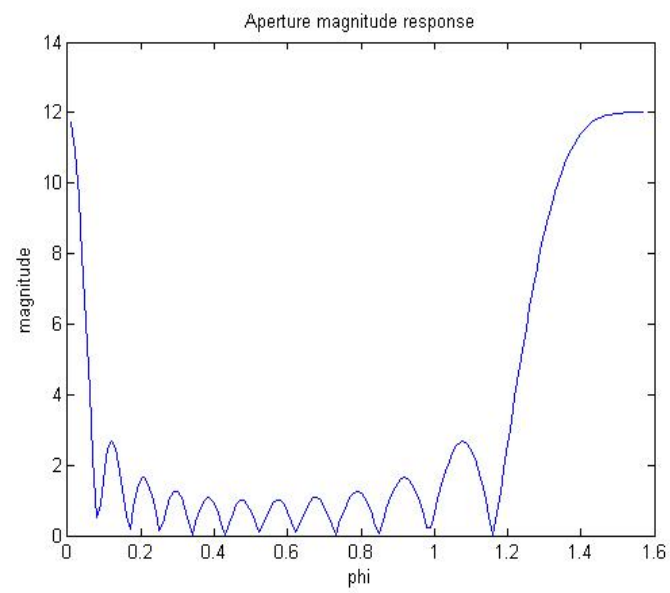


Figure 1.3: Spatial Aliasing

CHAPTER 2

Beamforming

Beamforming or spatial filtering is a technique used in sensor arrays for directional signal transmission or reception. This is achieved by combining elements in a sensor array such that signals from particular angles experience constructive interference while others experience destructive interference. Here we use beamforming to find the doa of signals by measuring the power received in every direction. Sensor arrays are capable of electronic steering i.e changing the look-direction for signals can be done electronically. This could not be achieved by conventional radars which mechanically rotate the antenna for changing the look-direction. In this section we discuss a time domain approach to beamforming and two spectrum based approaches.

Time domain - Delay-Sum beamformer

Spectrum based - Conventional (Bartlett) Beamformer and MVDR (Capon) beamformer.

2.1 Delay Sum Beamforming

Delay-Sum Beamforming Equation:

$$z(t) = \sum_{m=0}^{M-1} w_m y_m(t - \Delta_m)$$

w_m = shading done at m^{th} sensor

y_m = signal received by m^{th} sensor

Shading is external sensor gain provided at every sensor input. This is viewed as a spatial filter and is very similar to a time-domain filter. All kinds of filters used

in time-frequency domain like Chebyshev, kaiser, Blackmann etc. can be used here. In Fig. 1.2 it has a unity gain at all sensors i.e similar to a "rect" function in time-domain and "sinc" in frequency domain. This is the reason we see a "sinc" response in the wavenumber domain.

Plane wave Equation:

$$f(\vec{x}, t) = \exp(j(\omega_0 t - \vec{k}^0 \cdot \vec{x}))$$

$$f(\vec{x}, t) = s(t - \vec{\alpha}^0 \cdot \vec{x})$$

where $\vec{\alpha}^0 = \vec{k}^0 / \omega$

Beamformer Equation:

$$z(t) = \sum_{m=0}^{M-1} w_m y_m(t - \Delta_m - \vec{\alpha}^0 \cdot \vec{x}_m)$$

Therefore by choosing $\Delta_m = \vec{\alpha}^0 \cdot \vec{x}_m$ we get an undisturbed signal.

In general: $\Delta_m = \vec{\alpha} \cdot \vec{x}_m$, sweep $\vec{\alpha}$ to get the maximum power output from $z(t)$.

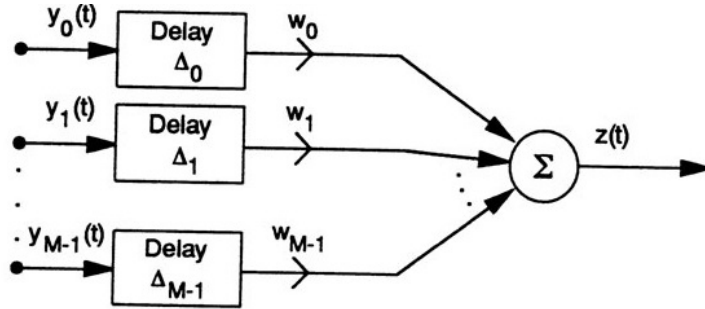


Figure 2.1: Delay-sum beamformer

2.2 Conventional Narrow band beamforming

Narrow band beamformer works when the input is a narrow band signal, where \vec{k}^0 or $\vec{\alpha}^0$ is a function of single wavelength. In wideband beamforming the steering vector is function of different wavelengths.

In narrowband case:

$$|\vec{k}| = \frac{2\pi}{\lambda}$$

Signal received by a single sensor:

$$y_m(t) = e^{-j\vec{k}^0 \cdot \vec{x}_m} s(t)$$

Vector notation:

$$\mathbf{y}(t) = \mathbf{e}(\vec{k}^0) s(t)$$

$$\begin{bmatrix} y_0(t) \\ y_1(t) \\ \vdots \\ y_{M-1}(t) \end{bmatrix} = \begin{bmatrix} \exp(-j\vec{k}^0 \cdot \vec{x}_0) \\ \exp(-j\vec{k}^0 \cdot \vec{x}_1) \\ \vdots \\ \exp(-j\vec{k}^0 \cdot \vec{x}_{M-1}) \end{bmatrix} s(t)$$

Narrow band beamformer equation:

$$z(t) = \sum_{m=0}^{M-1} w_m \exp j(\vec{k} - \vec{k}^0) \cdot \vec{x}_m s(t)$$

$$z(t) = e^H(\vec{k}) W e(\vec{k}^0) s(t)$$

Here "W" is a diagonal matrix of the shading parameters vector.

Power of the output becomes useful when handling Sampled data or snapshots.

$$P = |z(t)|^2 = e^H(\vec{k}) W y(t) y^H(t) W^H e(\vec{k})$$

Spatial Correlation Matrix:

$$R(t) = y(t) y^H(t)$$

$$P = |z(t)|^2 = e^H(\vec{k}) W R(y) W^H e(\vec{k})$$

Here, the beamformer sweeps all \vec{k} for the power spectrum. So, \vec{k} is known as a look vector and $e(\vec{k})$ is called steering vector.

2.3 Minimum Variance Distortionless Response (MVDR) Beamformer or Capon Beamformer:

Minimum Variance Cost function:

$$\hat{w} = \arg \min_{\mathbf{w}} w^H R_y w$$

Constraint:

$$e^H(\vec{k})w = 1$$

This is the "**Distortionless response**" constraint. It makes sure that signal in look direction is unaffected.

output: $z = w^H y$

If \vec{k} is the look direction and if there is any signal in that direction then it will be of the form $y = e(\vec{k})s$.

So, output: $z = w^H y = s$

since $e^H(\vec{k})w = w^H e(\vec{k}) = 1$

The solution for this constrained optimization is:

$$w(\vec{k}) = \frac{R_y^{-1} e(\vec{k})}{e^H(\vec{k}) R_y^{-1} e(\vec{k})}$$

output:

$$z = e^H(\vec{k}) \frac{R_y^{-1} e(\vec{k})}{e^H(\vec{k}) R_y^{-1} e(\vec{k})}$$

Output Power:

$$P_{mv} = \frac{1}{e^H(\vec{k}) R_y^{-1} e(\vec{k})}$$

whereas,

$$P_{conv} = e^H(\vec{k})R_y e(\vec{k})$$

2.4 Simulations

MVDR beamformer performs better than conventional beamformer. We can see the difference in Fig. 2.2 and Fig. 2.3.

In Fig. 2.2, received snr=5dB and two signals are coming from angles 30° and 100° with powers in the ratio of 1:2 respectively.

Fig. 2.3 has signals from the angles 30° and 60° where we can observe that conventional beamforming doesn't perform well due to its low resolution (large mainlobe width).

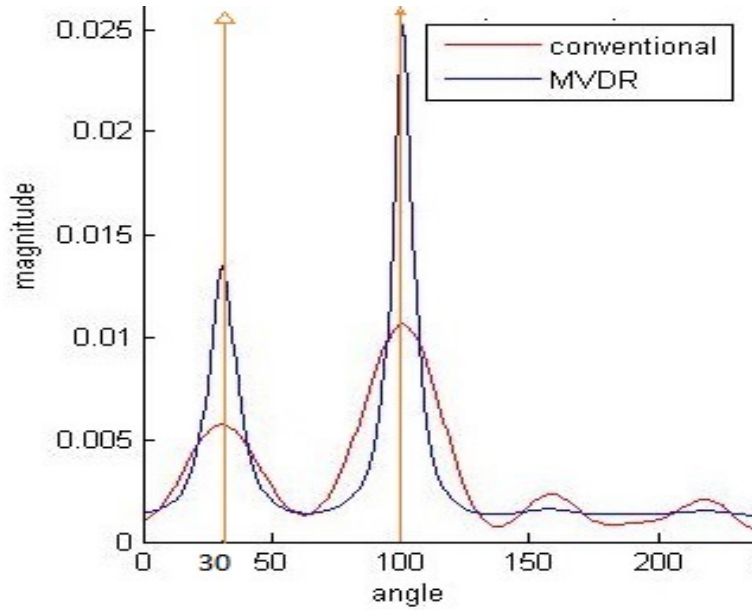


Figure 2.2: MVDR vs Conventional Beamformer, 9 sensors

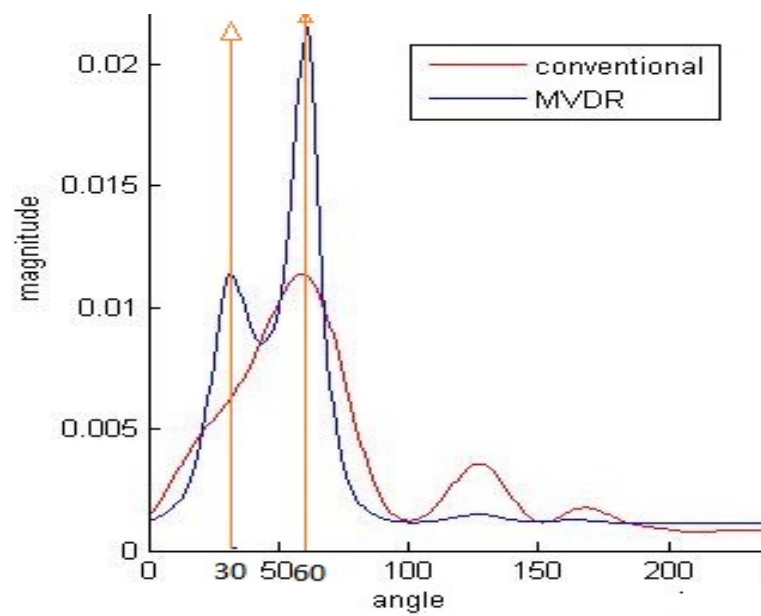


Figure 2.3: MVDR vs Conventional Beamformer, Resolution plot

CHAPTER 3

Subspace Methods

Here two high resolution methods based on eigenvalue decomposition techniques (subspace methods) are discussed.

- 1) Multiple Signal Classification (MUSIC)
- 2) Estimation of Signal Parameters via Rotational Invariance Technique (ESPRIT)

3.1 MUSIC

MUSIC stands for MUltiple Signal Classification, a subspace approach for resolving multiple signals. This concept is closely studied from this paper (Schmidt, 1986).

Data Model:

M sensor array

D sources are considered where $D < M$.

$$\begin{bmatrix} x_1 \\ x_2 \\ \vdots \\ \vdots \\ x_M \end{bmatrix} = \begin{bmatrix} a(\theta_1) & a(\theta_2) & \dots & a(\theta_D) \end{bmatrix} \begin{bmatrix} s_1 \\ s_2 \\ \vdots \\ \vdots \\ s_D \end{bmatrix} + \begin{bmatrix} n_1 \\ n_2 \\ \vdots \\ \vdots \\ n_M \end{bmatrix}$$

$$\mathbf{x}[k] = \mathbf{A}\mathbf{s}[k] + \mathbf{n}[k]$$

where

$\mathbf{x}[k]$ is the received vector at k^{th} snapshot,

\mathbf{s} is the input signal at the source, D sources are considered.

\mathbf{A} consists of columns that are steering vectors corresponding to each source.

\mathbf{n} is the noise vector.

Here, the array manifold \mathbf{A} which consists of steering vectors is represented in a different manner compared to the beamforming cases. Both are exactly same and the change in representation is done just for simplicity.

$a_i(\theta_j)$ corresponds to the j^{th} source and i^{th} element

$a_i(\theta_j) = e^{j(2\pi/\lambda)d_i \sin\theta_j}$ where d_i is position of the i^{th} element

Covariance Matrix:

$$\mathbf{R}_{xx} = \mathbf{x}\mathbf{x}^H = \mathbf{A}\mathbf{s}\mathbf{s}^H\mathbf{A}^H + \mathbf{n}\mathbf{n}^H$$

$$\mathbf{R}_{xx} = \mathbf{A}\mathbf{R}_{ss}\mathbf{A}^H + \mathbf{R}_{nn}$$

Let the noise covariance matrix be $\sigma^2\mathbf{I}$

$$\mathbf{R}_{xx} = \mathbf{A}\mathbf{R}_{ss}\mathbf{A}^H + \sigma^2\mathbf{I}$$

Since there are only D sources, the dimension of matrix \mathbf{R}_{ss} is D and the rank of $\mathbf{A}\mathbf{R}_{ss}\mathbf{A}^H$ is also D which is not full rank. From these facts, there are N=M-D eigen values of \mathbf{R}_{xx} which are equal to the noise variance σ^2 .

Let the noise eigenvectors matrix be \mathbf{E}_N . This is a $M \times N$ matrix. Music algorithm scans all directions and calculates $\mathbf{P}_{MUSIC}(\theta)$.

Therefore in the MUSIC algorithm,

$$\mathbf{P}_{MUSIC}(\theta) = \frac{1}{\mathbf{a}^H(\theta)\mathbf{E}_N\mathbf{E}_N^H\mathbf{a}(\theta)}$$

we find the peaks in this plot for the direction of arrival of sources.

3.1.1 Algorithm

- 1) Estimate \mathbf{R}_{xx} from snapshots
- 2) Calculate eigenvalues of \mathbf{R}_{xx} and decide number of signals D . Very low eigenvalues belong to noise.
- 3) Calculate $\mathbf{P}_{MUSIC}(\theta)$
- 4) pick D peaks in $\mathbf{P}_{MUSIC}(\theta)$. The angles corresponding to these are the estimated doa of sources.

3.1.2 Simulations

In the following plots, all the three beamforming methods are compared. In Fig. 3.1, received snr=5dB, and source signal angles of 30° and 100° . The high resolution performance of the MUSIC algorithm is evident.

In Fig. 3.2, the source signals are from angles 30° and 50° . In this case, mvdr and conventional beamforming methods fail because of their low resolution.

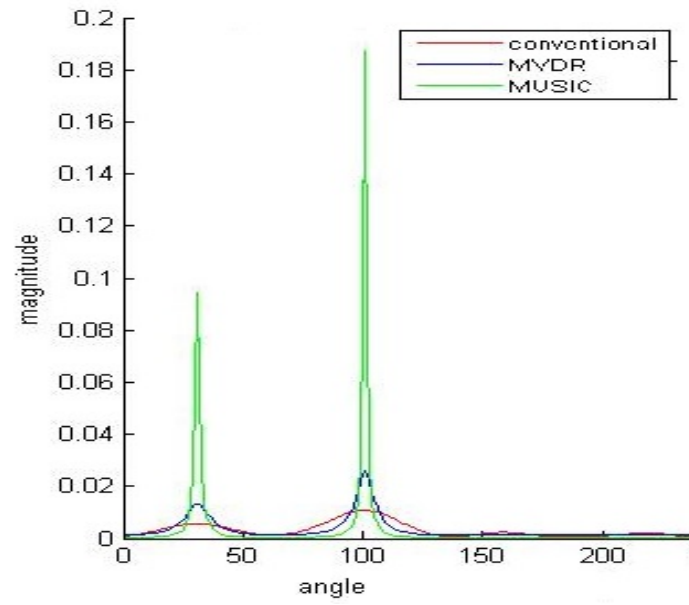


Figure 3.1: SNR = 5dB, Src angles = 30,100, 9 sensors

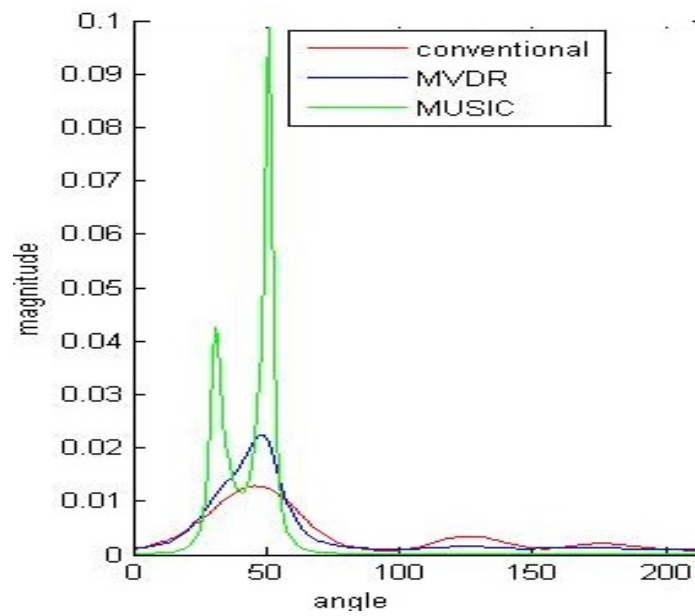


Figure 3.2: SNR = 5dB, Src angles = 30,50, 9 sensors

3.2 ESPRIT

ESPRIT- Estimation of Signal parameters via Rotational Invariance Technique. This method is similar to MUSIC and relies on eigenspace techniques. ESPRIT has less computational complexity when compared to MUSIC. But, this benefit is obtained with a compromise on the number of sensors. ESPRIT method requires double the number of sensors for achieving the same degrees of freedom as MUSIC. This concept is closely studied from (Roy and Kailath, 1989).

Signal Model:

M sensor array

D sources are considered where $D < M$.

$$\begin{bmatrix} x_1 \\ x_2 \\ \cdot \\ \cdot \\ \cdot \\ x_M \end{bmatrix} = \begin{bmatrix} a(\theta_1) & a(\theta_2) & \dots & a(\theta_D) \end{bmatrix} \begin{bmatrix} s_1 \\ s_2 \\ \cdot \\ \cdot \\ \cdot \\ s_D \end{bmatrix} + \begin{bmatrix} n_1 \\ n_2 \\ \cdot \\ \cdot \\ \cdot \\ n_M \end{bmatrix}$$

$$\mathbf{x}[k] = \mathbf{A}\mathbf{s}[k] + \mathbf{n}[k]$$

where

\mathbf{x} is the received vector,

\mathbf{s} is the input signal at the source, D sources are considered.

\mathbf{A} consists of columns that are mode vectors corresponding to each source.

\mathbf{n} is the noise vector.

This is similar to MUSIC algorithm. But in ESPRIT there is another set of sensors having the same structure as the latter but are shifted in position. This gives rise to doublets. Every sensor in one set has its pair in the other set.

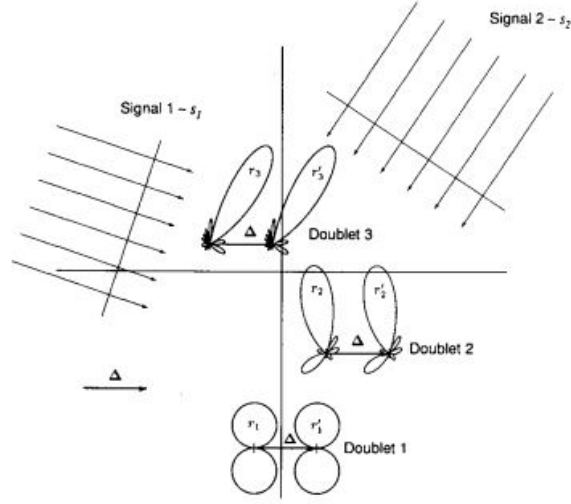


Figure 3.3: ESPRIT sensor array geometry

Core idea of ESPRIT - Rotational Invariance:

Let the position of i^{th} sensor in set-1 be \vec{p}_i and position i^{th} sensor in set-2 be \vec{q}_i .

$$\vec{q}_i = \vec{p}_i + \vec{\Delta}$$

From the figure, the signal received at \vec{q}_i is a delayed version of the signal at \vec{p}_i . This delay is dependent on the direction of arrival of the source signal. ESPRIT algorithms estimates this delay to find the direction of arrival.

Let the signals received at the i th doublet be:

$$x_i(t) = \sum_{k=1}^d s_k(t) a_i(\theta_k) + n_{x_i}(t)$$

$$y_i(t) = \sum_{k=1}^d s_k(t) e^{j\omega_0 \Delta \sin \theta_k / c} a_i(\theta_k) + n_{y_i}(t)$$

The exponential part in the second equation is the rotation vector. Hence the name rotational invariance.

Vector representation:

$$\mathbf{x}[k] = \mathbf{A}\mathbf{s}[k] + \mathbf{n}[k]$$

$$\mathbf{y}[k] = \mathbf{A}\boldsymbol{\phi}\mathbf{s}[k] + \mathbf{n}[k]$$

$$\boldsymbol{\phi} = \text{diag}(e^{j\gamma_1}, \dots, e^{j\gamma_d})$$

where $\gamma = \omega_0 \Delta \sin \theta_k / c$

The objective is to estimate $\boldsymbol{\phi}$ and thereby obtaining the source angles in one shot. This is in contrast to MUSIC where the algorithm looks in every direction for calculating doa. ESPRIT can estimate doa directly from $\boldsymbol{\phi}$ and is therefore considerably faster than MUSIC.

3.2.1 Algorithm

1) Define

$$\mathbf{z}[k] = \begin{bmatrix} \mathbf{x}[k] \\ \mathbf{y}[k] \end{bmatrix} = \begin{bmatrix} \mathbf{A} \\ \mathbf{A}\boldsymbol{\phi} \end{bmatrix} \mathbf{s}[k] + \begin{bmatrix} \mathbf{n}_x[k] \\ \mathbf{n}_y[k] \end{bmatrix} = \bar{\mathbf{A}}\mathbf{s}[k] + \mathbf{n}_z[k]$$

Compute the $2N \times 2N$ correlation matrix \mathbf{R}_{zz}

$$\mathbf{R}_{zz} = \bar{\mathbf{A}}\mathbf{R}_{ss}\bar{\mathbf{A}}^H + \sigma_0^2\mathbf{I}$$

2) Since there are D sources, the D largest eigenvectors of \mathbf{R}_{zz} form the signal subspace \mathbf{U}_s . The remaining $2N-D$ eigenvectors form the noise subspace \mathbf{U}_n .

\mathbf{U}_s is $2N \times D$ and its span is same as $\bar{\mathbf{A}}$

Therefore there exists a transformation matrix \mathbf{T} such that

$$\mathbf{U}_s = \bar{\mathbf{A}}\mathbf{T}$$

Now, partition \mathbf{U}_s into two $N \times D$ matrices.

$$\mathbf{U}_s = \begin{bmatrix} \mathbf{U}_x \\ \mathbf{U}_y \end{bmatrix} = \begin{bmatrix} \mathbf{A}\mathbf{T} \\ \mathbf{A}\phi\mathbf{T} \end{bmatrix}$$

Observe that the columns of both \mathbf{U}_x and \mathbf{U}_y are linear combinations of \mathbf{A} , so both of them should have rank D .

3) Define an $N \times 2D$ matrix, which has rank D

$$\mathbf{U}_{xy} = \begin{bmatrix} \mathbf{U}_x & \mathbf{U}_y \end{bmatrix}$$

Therefore, \mathbf{U}_{xy} has a null space with dimension D , so there exists a $2D \times D$ matrix \mathbf{F} such that

$$\mathbf{U}_{xy}\mathbf{F} = 0 = \begin{bmatrix} \mathbf{U}_x & \mathbf{U}_y \end{bmatrix} \begin{bmatrix} \mathbf{F}_x \\ \mathbf{F}_y \end{bmatrix} = \mathbf{U}_x\mathbf{F}_x + \mathbf{U}_y\mathbf{F}_y = 0$$

Solving the above equation we get,

$$\phi = \mathbf{T}\mathbf{F}_x\mathbf{F}_y^{-1}\mathbf{T}^{-1}$$

4) Let $\psi = \mathbf{F}_x\mathbf{F}_y^{-1}$.

ψ and ϕ share the same eigenvalues. Therefore, ϕ can be estimated by finding the eigenvalues of ψ . This is a least-squares ESPRIT method. Total least squares (TLS-ESPRIT) is applied for better performance.

3.2.2 Simulations

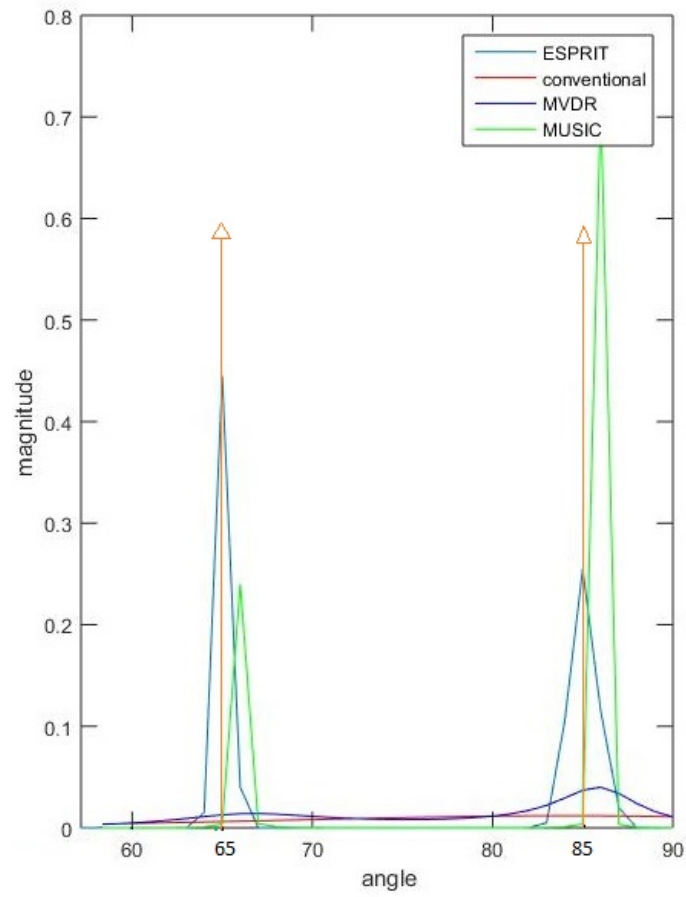


Figure 3.4: SNR=10dB, 9 sensors, ESPRIT = 18 sensors, angles = 65,85

CHAPTER 4

Nested Arrays

Recent work on Nested arrays (Pal and Vaidyanathan, 2010) has gained significant fame in the field of array signal processing. In their paper, a new array geometry named Nested arrays is developed through which it is possible to detect $O(N^2)$ sources with only N sensors. An algorithm based on spatial smoothing and MUSIC for nested arrays has been mentioned in (Pal and Vaidyanathan, 2010). In this chapter a new algorithm using spatial smoothing and ESPRIT is developed and compare both the results. We will show that ESPRIT is considerably faster than MUSIC while maintaining almost the same RMSE. Spatial smoothing techniques which include Forward smoothing and Forward-Backward smoothing are referred from (Pillai and Kwon, 1989).

Data Model:

M sensor array

D sources are considered where $D < M$.

$$\begin{bmatrix} x_1 \\ x_2 \\ \cdot \\ \cdot \\ \cdot \\ x_M \end{bmatrix} = \begin{bmatrix} a(\theta_1) & a(\theta_2) & \dots & a(\theta_D) \end{bmatrix} \begin{bmatrix} s_1 \\ s_2 \\ \cdot \\ \cdot \\ \cdot \\ s_D \end{bmatrix} + \begin{bmatrix} n_1 \\ n_2 \\ \cdot \\ \cdot \\ \cdot \\ n_M \end{bmatrix}$$

$$\mathbf{x}[k] = \mathbf{A}\mathbf{s}[k] + \mathbf{n}[k]$$

where

$\mathbf{x}[k]$ is the received vector at k^{th} snapshot,

\mathbf{s} is the input signal at the source, D sources are considered.

\mathbf{A} consists of columns that are steering vectors corresponding to each source.

\mathbf{n} is the noise vector.

$a_i(\theta_j) = e^{j(2\pi/\lambda)d_i \sin\theta_j}$ where d_i is position of the i^{th} element

Covariance Matrix:

$$\mathbf{R}_{xx} = \mathbf{x}\mathbf{x}^H = \mathbf{A}\mathbf{s}\mathbf{s}^H\mathbf{A}^H + \mathbf{n}\mathbf{n}^H$$

$$\mathbf{R}_{xx} = \mathbf{A}\mathbf{R}_{ss}\mathbf{A}^H + \mathbf{R}_{nn}$$

Let the noise covariance matrix be $\sigma^2 \mathbf{I}$

$$\mathbf{R}_{xx} = \mathbf{A}\mathbf{R}_{ss}\mathbf{A}^H + \sigma^2 \mathbf{I}$$

Now vectorize \mathbf{R}_{xx} to get the following vector:

$$\begin{aligned} \mathbf{z} = \text{vec}(\mathbf{R}_{xx}) &= \text{vec}\left[\sum_{i=1}^D \sigma_i^2 \mathbf{a}(\theta_i) \mathbf{a}^H(\theta_i)\right] + \sigma^2 \vec{\mathbf{1}}_m \\ &= (\mathbf{A}^* \odot \mathbf{A})\mathbf{p} + \sigma^2 \vec{\mathbf{1}}_m \end{aligned} \quad (4.1)$$

where $\mathbf{p} = [\sigma_1^2 \ \sigma_2^2 \ \dots \ \sigma_D^2]$ and $\vec{\mathbf{1}}_m = [e_1^T \ e_2^T \ \dots \ e_N^T]$ where e_i being a column vector of all zeros except a 1 at i th position. Comparing (4.1) with the standard receiver signal model, \mathbf{z} in (4.1) behaves like the received signal by an array whose manifold is given by $\mathbf{A}^* \odot \mathbf{A}$ where \odot denoted KR-product. The equivalent source signal vector is represented by \mathbf{p} which does not change with time. The noise becomes a deterministic vector given by $\sigma^2 \vec{\mathbf{1}}_m$. The distinct rows in $\mathbf{A}^* \odot \mathbf{A}$ behave like the manifold of a longer uniform linear array whose positions are at $\vec{x}_i - \vec{x}_j, 1 \leq i, j \leq M$ where \vec{x}_i denotes the position of the i th sensor in the original array. We call this long longer array as a difference coarray. Hence, we can apply DOA estimation techniques like MUSIC and ESPRIT on

this difference co-array.

4.1 Algorithm Formulation

Here we consider a 2-level nested array as proposed in (Pal and Vaidyanathan, 2010) which has $M/2$ sensors in each level. Here we assume M to be even. An example of a 2-level nested array with 6 sensors is shown in Fig. 4.2. Consider equation (4.3),

$$\mathbf{z} = (\mathbf{A}^* \odot \mathbf{A})\mathbf{p} + \sigma^2 \vec{\mathbf{1}}_m$$

where $\mathbf{p} = [\sigma_1^2 \ \sigma_2^2 \ \dots \ \sigma_D^2]$. The source correlation matrix \mathbf{R}_{pp} will have rank 1 i.e the sources are completely correlated. Spatial smoothing is a well-known technique used to de-correlate coherent sources. It is to be noted that spatial smoothing technique is applicable only to ULAs.

Before applying spatial smoothing, a new matrix \mathbf{A}_r of size $((M^2 - 2)/2 + M) \times D$ is constructed from $\mathbf{A}^* \odot \mathbf{A}$ where the repeated rows are removed after their first occurrence. After that the rows are sorted such that the i th row corresponds to the sensor location $(-M^2/4 - M/2 + i)d$ in the difference co-array of the 2-level nested array.

The new vector \mathbf{z}_r is given by

$$\mathbf{z}_r = \mathbf{A}_r \mathbf{p} + \sigma^2 \mathbf{e}'$$

where $\mathbf{e}' \in \mathbf{R}^{((M^2-2)/2+M) \times 1}$ is a vector of all zeros except a 1 at $(M^2/4 + M/2)$ th position.

In the above equation, the positions of the sensors are same as the difference co-array which is a ULA. The sensors are located from $(-M^2/4 - M/2 + 1)d$ to $(M^2/4 + M/2 - 1)d$. We divide this co-array into

$M^2/4 + M/2$ overlapping subarrays, each with $(M^2/4 + M/2)$ elements, where the i th subarray has sensors located at

$$\{(-i + 1 + m)d, m = 0, 1, \dots, (M^2/4 + M/2 - 1)\}$$

Now, we apply spatial smoothing on these subarrays to get the spatially smoothed covariance matrix.

Let \mathbf{z}_i be the received vector by the i^{th} subarray.

$$\mathbf{z}_i = \mathbf{A}_i \mathbf{p} + \sigma^2 \mathbf{e}_i$$

where \mathbf{A}_i is the manifold matrix corresponding to the i^{th} subarray and \mathbf{e}_i is an all zero vector with a 1 in the i^{th} position. It is easy to observe that the array manifold of the i^{th} subarray can be represented using the manifold of the first subarray.

$$\mathbf{A}_i = \mathbf{A}_1 \boldsymbol{\phi}^{i-1}$$

where

$$\boldsymbol{\phi} = \text{diag}(e^{-j(2\pi/\lambda)d \sin(\theta_1)}, e^{-j(2\pi/\lambda)d \sin(\theta_2)}, \dots, e^{-j(2\pi/\lambda)d \sin(\theta_D)})$$

Therefore,

$$\mathbf{z}_i = \mathbf{A}_1 \boldsymbol{\phi}^{i-1} \mathbf{p} + \sigma^2 \mathbf{e}_i$$

The subarray covariance matrix \mathbf{R}_i is

$$\mathbf{R}_i = \mathbf{z}_i \mathbf{z}_i^H = \mathbf{A}_1 \phi^{i-1} \mathbf{p} \mathbf{p}^H (\phi^{i-1})^H \mathbf{A}_1^H + \sigma_m^4 \mathbf{e}_i \mathbf{e}_i^H + \sigma^2 \mathbf{A}_1 \phi^{i-1} \mathbf{p} \mathbf{e}_i^H + \sigma^2 \mathbf{e}_i \mathbf{p}^H (\phi^{i-1})^H \mathbf{A}_1^H$$

Averaging over all subarray covariance matrices we get the spatially smoothed covariance matrix R_s .

$$R_s = \frac{1}{\left(\frac{M^2}{4} + \frac{M}{2}\right)} \sum_{i=1}^{M^2/4+M/2} R_i$$

It is proved in (Pal and Vaidyanathan, 2010) that $R_s = \hat{R}^2$ where

$$\hat{R} = \frac{1}{\sqrt{\frac{M^2}{4} + \frac{M}{2}}} (A_{11} \Lambda A_{11}^H + \sigma^2 I)$$

has the same form as the covariance matrix of the signal received by a ULA consisting of $M^2/4 + M/2$ sensors.

\hat{R} and R_s share the same set of eigenvectors and the eigenvalues of \hat{R} are the square roots of those of R_s .

We apply ESPRIT algorithm on this covariance matrix to detect upto $M^2/4 + M/2 - 2$ sources.

The rank of the new covariance matrix is equal to the dimension of the source covariance matrix. Spatial smoothing de-correlates the sources and hence the source correlation matrix has full rank. Now, for the purpose of using ESPRIT we need two shifted arrays. Two shifted subarrays each of length

$(M^2/4 + M/2 - 1)$ are considered for this purpose. Let

$$M^+ = (M^2/4 + M/2 - 1)$$

Let $\mathbf{x}[k]$ and $\mathbf{y}[k]$ denote the received vectors at the first and second subarrays

respectively at the k^{th} snapshot. Also, let \mathbf{A} be the array manifold of the first sub-array

$$\mathbf{x}[k] = \mathbf{A}\mathbf{s}[k] + \mathbf{n}_x[k]$$

$$\mathbf{y}[k] = \mathbf{A}\phi\mathbf{s}[k] + \mathbf{n}_y[k]$$

where

$$\phi = \text{diag}(e^{-j(2\pi/\lambda)d \sin(\theta_1)}, e^{-j(2\pi/\lambda)d \sin(\theta_2)}, \dots, e^{-j(2\pi/\lambda)d \sin(\theta_D)})$$

After vertical concatenation of both the vectors we get,

$$\begin{aligned} \mathbf{z} = \begin{bmatrix} \mathbf{x}[k] \\ \mathbf{y}[k] \end{bmatrix} &= \begin{bmatrix} \mathbf{A} \\ \mathbf{A}\phi \end{bmatrix} \mathbf{s}[k] + \begin{bmatrix} \mathbf{n}_x[k] \\ \mathbf{n}_y[k] \end{bmatrix} \\ &= \bar{\mathbf{A}}\mathbf{s}[k] + \mathbf{n}_z[k] \end{aligned}$$

The covariance matrix \mathbf{R}_{zz} of size $M^+ \times M^+$ can be easily constructed as covariance between any two sensors is known from \mathbf{R}_s .

$$\mathbf{R}_{zz} = \bar{\mathbf{A}}\mathbf{R}_s\bar{\mathbf{A}}^H + \sigma_0^2\mathbf{I}$$

We apply TLS-ESPRIT on this $M^+ \times M^+$ matrix to detect upto $M^+ - 1$ sources.

4.2 Simulation System Model

4.2.1 Sensor Array Structure

A 6 sensor 2-level nested array ($M = 6$) is considered with 8 narrowband sources ($D = 8$) impinging on it from angles $[-60, -40, -20, 0, 10, 35, 50, 65]$ with respect to the normal of the sensor array. The sources are modeled as random Gaussian processes with equal power. This 2-level nested array has 3 sensors in each level. The method based on spatial smoothing and MUSIC proposed in (Pal and Vaidyanathan, 2010) can resolve upto $M^2/4 + M/2 - 1 = 11$ sources and the method proposed using ESPRIT in this paper can resolve upto $M^2/4 + M/2 - 2 = 10$. In the following simulations instead of MUSIC and LS-ESPRIT we implement rootMUSIC and TLS-ESPRIT because the latter give better performances.

Sensors are placed at distances 1,2,3,4,8,12 on y-axis from the origin as shown in Fig. 4.1.

4.2.2 Co-Array structure

From Fig. 4.2, we can see that the difference co-array gives rise to an ULA with 23 unique sensors.

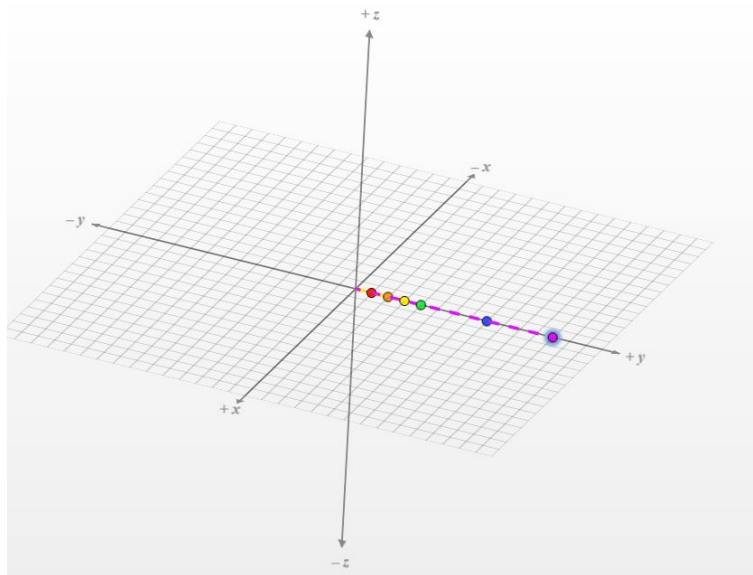


Figure 4.1: Nested Array

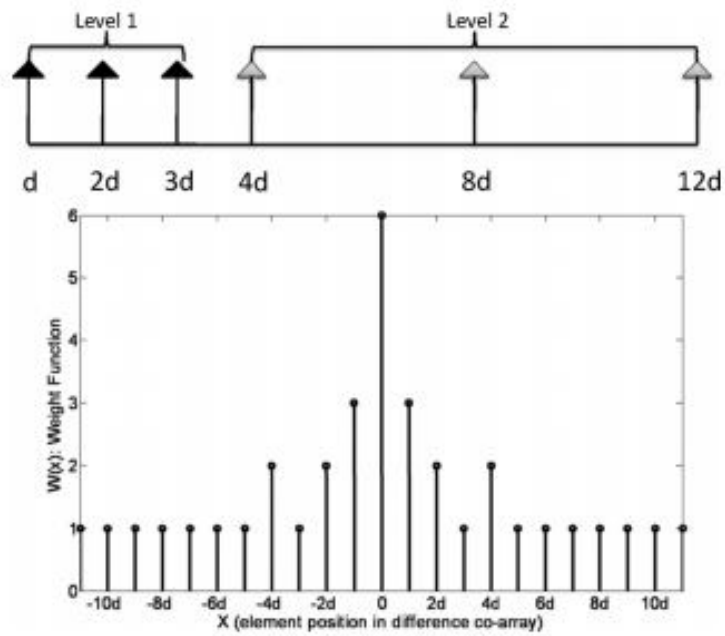


Figure 4.2: Co-Array

4.3 Simulations

Angle plots

Fig. 4.3 shows the angle plots with both rootMUSIC and ESPRIT applied on nested arrays. Both use $T = 9600$ snapshots and $\text{SNR} = 0$ dB. Since rootMUSIC and ESPRIT directly spit out the angles, we take a histogram of the angles after running it for 500 times for the purpose of plotting. The bin size of the histogram is taken to be $1/1000$. From the figure, it can be seen that both the algorithms resolve the sources reasonably well. Note that SS-rootMUSIC means spatial smoothing and rootMUSIC are used in the algorithm and similarly SS-ESPRIT means spatial smoothing and ESPRIT are used.

Fig. 4.4 shows similar plots but with $T = 800$ snapshots and with $\text{SNR} = 0$ dB. We can clearly observe that the variance of the estimates increased as number of snapshots reduced.

RMSE vs SNR

Here we compare the root mean squared error (RMSE) of both the algorithms. We average over 1000 Monte Carlo simulations and $T = 9600$ snapshots are used for Fig. 4.5. We have $T = 800$ snapshots for Fig. 4.6. Also, we compare both algorithms with a 12-element ULA response which uses rootMUSIC for doa estimation. From both the figures we can observe that both the algorithms give almost same performance w.r.t RMSE.

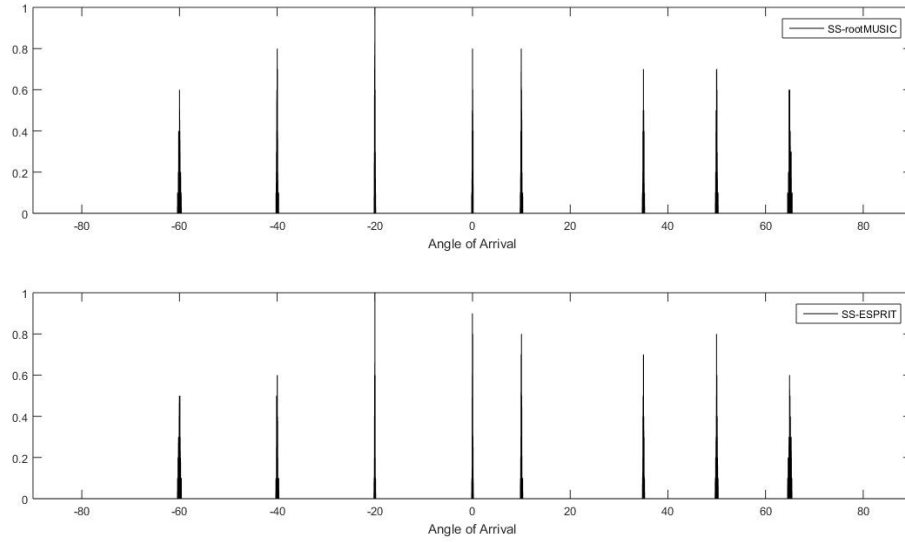


Figure 4.3: Histogram of source angles observed by 6 element nested array with SS-rootMUSIC and SS-ESPRIT algorithms, $T = 9600$

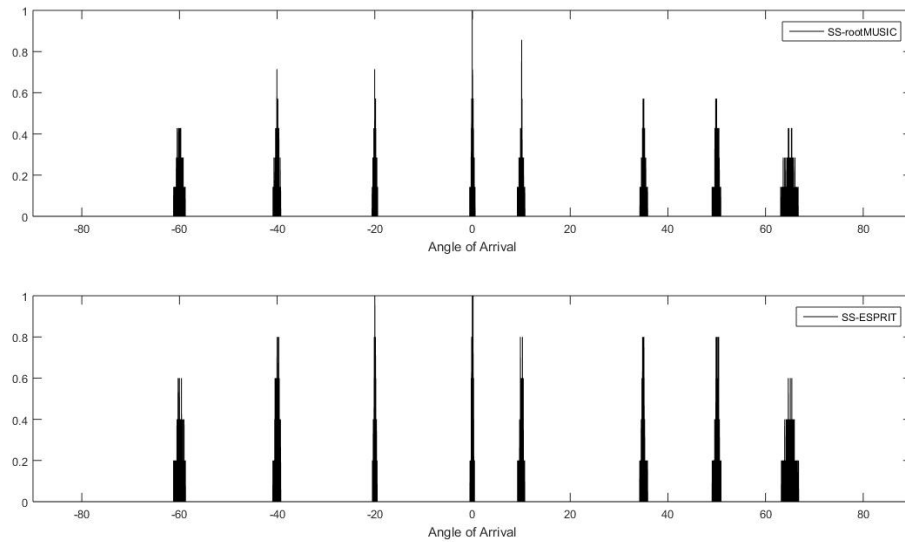


Figure 4.4: Histogram of source angles observed by 6 element nested array with SS-rootMUSIC and SS-ESPRIT algorithms, $T = 800$

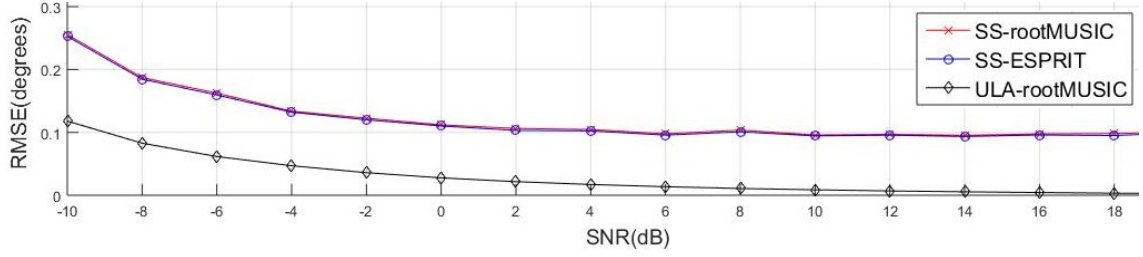


Figure 4.5: RMSE of source angles w.r.t SNR as observed by a 6 element nested array with SS-rootMUSIC and SS-ESPRIT algorithms and as observed by a 12-element ULA with rootMUSIC algorithm, $T = 9600$

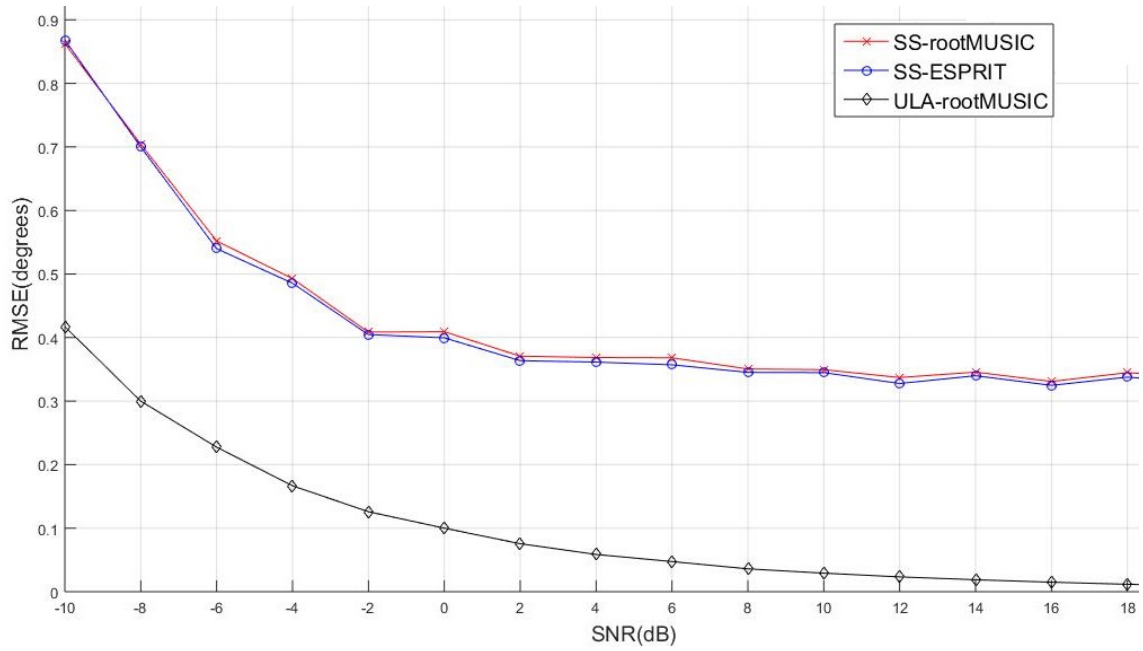


Figure 4.6: RMSE of source angles w.r.t SNR as observed by a 6 element nested array with SS-rootMUSIC and SS-ESPRIT algorithms and as observed by a 12-element ULA with rootMUSIC algorithm, $T = 800$

Time taken by algorithm vs snapshots

Here we calculate the time taken by each algorithm for some specific values of snapshots and compare both the algorithms. SNR = 0 dB and the elapsed time is averaged over 1000 Monte Carlo simulations. We can observe the benefit of using ESPRIT algorithm over rootMUSIC from Fig. 4.7 because ESPRIT is considerably faster than rootMUSIC. Note that we may not observe the increase in elapsed time w.r.t to snapshots because the elapsed time is calculated after estimating the covariance matrices.

Fig. 4.8 includes the time taken to calculate of covariance matrices and hence we can see the increase in time taken.

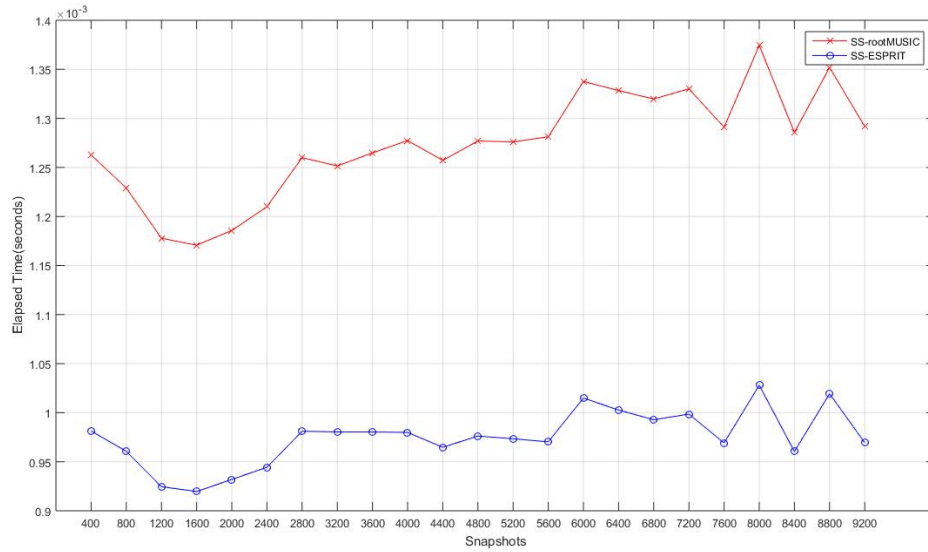


Figure 4.7: Time taken by both the algorithms after feeding in the covariance matrices. ESPRIT is faster than rootMUSIC.

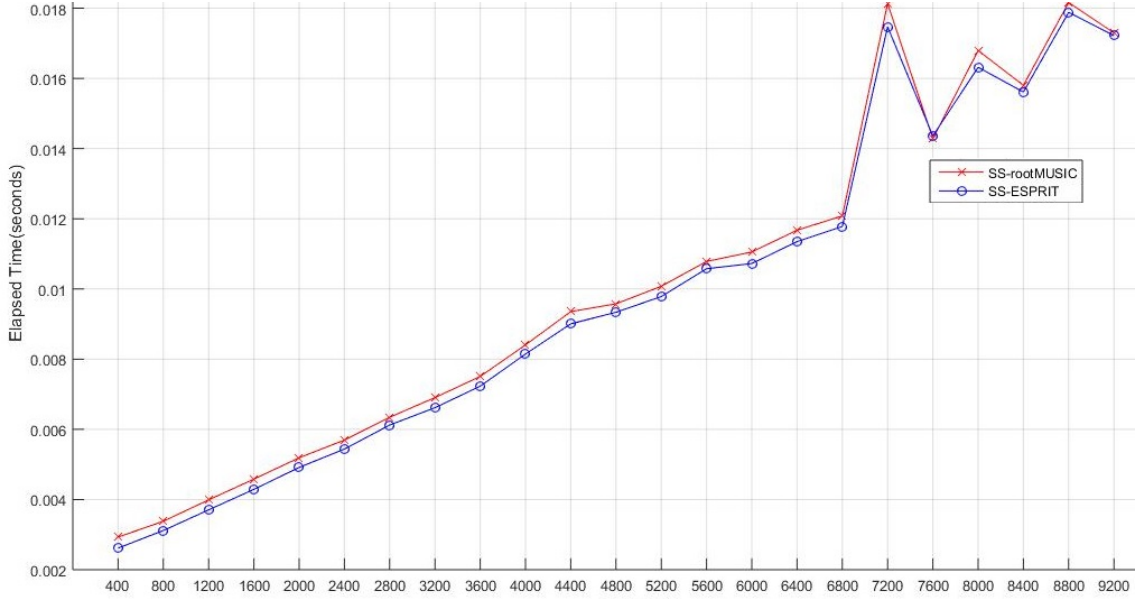


Figure 4.8: Time taken by both the algorithms which includes the estimation of covariance matrices also. ESPRIT is faster than rootMUSIC.

Nested Arrays vs ULA

Although nested arrays are used for finding direction of arrivals of $O(N^2)$ sources which is not possible with ULA's, here we consider an example of finding doa of less than N sources. We show that using nested array with 6 sensors results in considerably less RMSE than using a ULA with 6 sensors. Nested array has sensors at positions [1 2 3 4 8 12] on the y-axis whereas ULA has sensors at [1 2 3 4 5 6] on the y-axis. The number of snapshots $T = 9600$. rootMUSIC and ESPRIT algorithms are applied on the ULA and SS-rootMUSIC and SS-ESPRIT are applied on the nested array as mentioned in the previous sections. The RMSE is averaged over 1000 Monte Carlo simulations. From Fig. 4.9, we can observe that RMSE for nested arrays is significantly lower than that of ULA at lower SNR's.

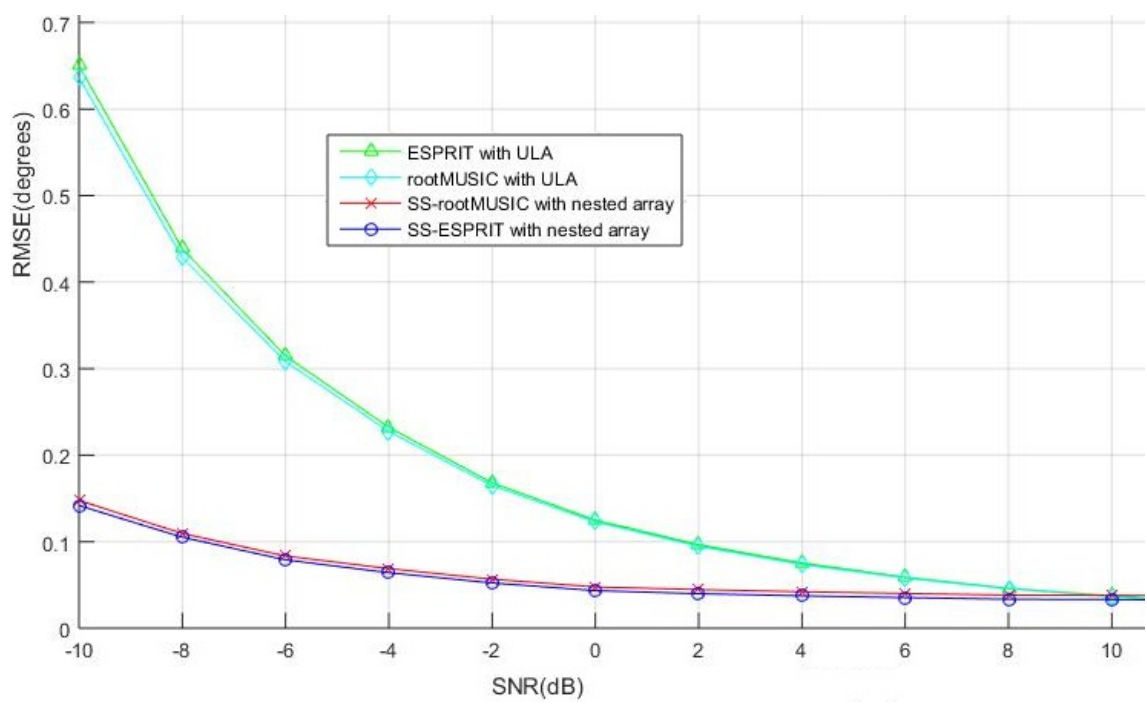


Figure 4.9: RMSE performance comparison between ULA and Nested array with 6 sensors each.

4.3.1 Conclusions

From Fig. 4.5 and Fig. 4.6 we can observe that RMSE is almost same for both the algorithms. Infact, an experiment in (Roy and Kailath, 1989) showed that even though doa from MUSIC has less variance compared to ESPRIT, it suffers from high bias whereas ESPRIT results in very low bias. We can observe the algorithmic time benefits of using ESPRIT over MUSIC from Fig. 4.7. Also, from Fig. 4.9 we observe the benefits of using a nested array over ULA in general.

REFERENCES

1. **Johnson, D. H.** and **D. E. Dudgeon**, *Array signal processing: concepts and techniques*. Simon & Schuster, 1992.
2. **Pal, P.** and **P. Vaidyanathan** (2010). Nested arrays: a novel approach to array processing with enhanced degrees of freedom. *Signal Processing, IEEE Transactions on*, **58**(8), 4167–4181.
3. **Pillai, S. U.** and **B. H. Kwon** (1989). Forward/backward spatial smoothing techniques for coherent signal identification. *Acoustics, Speech and Signal Processing, IEEE Transactions on*, **37**(1), 8–15.
4. **Roy, R.** and **T. Kailath** (1989). Esprit-estimation of signal parameters via rotational invariance techniques. *Acoustics, Speech and Signal Processing, IEEE Transactions on*, **37**(7), 984–995.
5. **Schmidt, R. O.** (1986). Multiple emitter location and signal parameter estimation. *Antennas and Propagation, IEEE Transactions on*, **34**(3), 276–280.
6. **Van Trees, H. L.**, *Detection, estimation, and modulation theory, optimum array processing*. John Wiley & Sons, 2004.